Evaluation of antifungal activity and potential application as fluorescent probes of indolenine and benzo[*e*]indole-based squarylium dyes

Vanessa S. D. Gomes[a,b], João C. C. Ferreira[b,c,d], Renato E. Boto[e], Paulo Almeida[e], José R. Fernandes[f], Maria João Sousa[c,d], Lucinda V. Reis[a,*] and M. S. T. Gonçalves[b,*]

[a] *Centre of Chemistry -Vila Real (CQ-VR) / Department of Chemistry, University of Trás-os-Montes and Alto Douro, Quinta de Prados, 5001-801, Vila Real, Portugal.*

[b] *Centre of Chemistry (CQ-UM) / Department of Chemistry, University of Minho, Campus of Gualtar, 4710-057 Braga, Portugal*

[c] *Centre of Molecular and Environmental Biology (CBMA) / Department of Biology, University of Minho, Campus of Gualtar, 4710-057 Braga, Portugal.*

[d] *Institute of Science and Innovation for Bio-Sustainability (IBS), University of Minho, Campus of Gualtar, 4710-057 Braga., Portugal.*

[e] *Health Sciences Research Centre (CICS-UBI) / Department of Chemistry, University of Beira Interior, Av. Infante D. Henrique, 6201-506 Covilhã, Portugal.*

[f] *Centre of Chemistry -Vila Real (CQ-VR) / Physical Department, University of Trás-os-Montes and Alto Douro, Quinta de Prados, 5001-801, Vila Real, Portugal*

**** Correspondence:*** *lucinda.reis@utad.pt; msameiro@quimica.uminho.pt*

Keywords: ▪ Squarylium dyes ▪ Singlet oxygen ▪ Photostability ▪ Antifungal agents ▪ Photodynamic Effect ▪ Fluorescence probes ▪Human Serum Albumin

Abstract: The antifungal performance and the possible use as fluorescent probes of a series of squarylium dyes derived from indolenine and benzo[*e*]indole previously synthesized was evaluated. Some photophysical properties were performed in ethanol and phosphate buffer, and the type of aggregates form in phosphate buffer was analyzed. Using the 1,3-diphenylisobenzofuran assay, a qualitative assessment of the capacity of dyes to produce singlet oxygen after irradiation was performed. Regarding the antifungal activity, this was studied through a broth microdilution assay using *Saccharomyces cerevisiae* PYCC 4072 as a biological model. The effect of irradiation of the dyes, with an appropriate light emitting diode system,

on the antifungal activity was also evaluated, and it was verified that some of the dyes improve their activity after irradiation. Using fluorescence microscopy techniques, the colocalization of dyes in *S. cerevisae* cells was investigated and it was possible to verify that some of the squarylium dyes with a barbituric moiety in the four-membered central ring stained and accumulated preferentially in the mitochondrial web and perinuclear membrane of the cells. The possible use as a fluorescent probe for the detection of HSA was also evaluated for one of the dyes of the series, demonstrating a linear variation of the fluorescence intensity accompanied by the increase of the protein concentration.

1. Introduction

Since the first reports in the history of humanity, society has suffered from various diseases of infectious origin constituting one of the main causes of mortality. Currently, fungal infections continue to be an emerging problem that has increased exponentially in recent decades, and is still responsible for over one-third of deaths worldwide [1, 2]. A healthy individual is able to cohabitate with disease-causing fungal agents, but when there is a breakdown of the immune system or high exposure to these agents, an infectious disease is triggered that can be asymptomatic or can rapidly progress to a lethal systemic disease [3-5].

The successful treatment of these diseases is essentially based on rapid diagnosis and the application of an antifungal agent that acts quickly and effectively. Despite the existence of clinically approved antifungal agents for the treatment of infectious diseases, they reveal some disadvantages that are based on the long duration of the treatments, the high toxicity that leads to undesirable side effects also the development of fungal resistance to the action of these antifungal agents [6, 7]. Faced with this problem, the search for antifungal agents or combination therapies for the treatment of infectious diseases is a challenging and essential area in constant development.

A class of dyes that has been developed in order to be applied in both biological and technological applications are the squarylium dyes [8, 9]. As a result of the conjugated π-system these dyes present some photophysical features such as narrow and intense bands ranging from the red to near infrared (NIR) region [10-12], moderate fluorescence quantum yields, high molar extinction coefficients [13, 14] and the moderate ability to generate singlet oxygen [15] make these dyes so applied in the most diverse areas.

One of the applications of compounds of the squarylium dye class that has been widely explored is their use as photosensitizers in photodynamic therapy [16, 17]. Based on this type of application, some authors have tested the photosensitizing character of squarylium dyes with different structural alterations against tumor cells [12, 18, 19] and bacteria [20, 21] demonstrating the strong potential of this class of dyes in these types of photodynamic therapy. The use of squaraine dyes in antifungal photodynamic therapy is still little explored, but the need for new antifungal agents and the good results showed by squaraine dyes in types of photodynamic therapy previously addressed, suggest that they may also be effective like antifungal agents.

The dyes presented in this work are shown in Figure 1 and their synthesis has already been reported by our research group [22-25] . The activity as antifungal agents against *Saccharomyces cerevisiae* of some of the presented dyes (**SQ5**, **6** and **SQ8**, **9**) has also been evaluated in previously published studies [25]. Thus, in this work, the evaluation of antifungal activity of dyes **SQ1**-**4** and **SQ7** against *S. cerevisiae* yeast will be carried out, as well as other complementary studies such as photosensitivity and singlet oxygen production, in order to be able to compare the different response caused by changes in the structure of the dyes.

The detection of bovine serum albumin (HSA) using squarylium dyes as fluorescent probes is also one of the applications already investigated for the presented dyes, except dye **SQ7**, which was studied as a potential fluorescent probe for the detection of HSA for the first time, in order to be able to compare its structure-activity relationship with the other dyes already evaluated [23-25].

A new study was also introduced to evaluate the location and distribution of dyes in cells in order to understand if the antifungal activity of each dye is related to its different distribution at the cellular level, thus allowing to obtain more information about the structural-activity relationship. On the other hand, another objective is to evaluate the possible use of these dyes as fluorescent markers of specific cellular organelles, and in this way introduce a new potential application of these dyes.

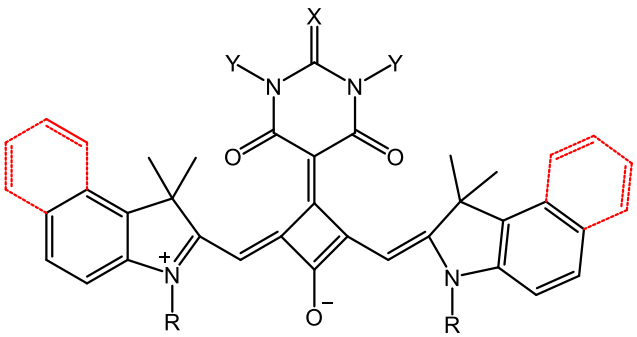

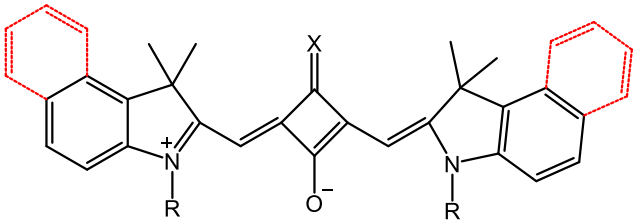

1: X = O; R = $(CH_2)_5CH_3$; Y = H
2: X = S; R = $(CH_2)_5CH_3$; Y = H
3: X = O; R = $(CH_2)_5CH_3$; Y = CH_3
4: X = S; R = $(CH_2)_5CH_3$;Y = C_6H_5
5: X = O; R = $(CH_2)_5CH_3$; Y = H
6: X = S; R = $(CH_2)_5CH_3$; Y = H

7: X = O; R=H
8: X = O; R=$(CH_2)_2COO(CH_2)_3CH_3$
9: X = O; R=$(CH_2)_2COO(CH_2)_3CH_3$

Figure 1. Squaraine dyes (**SQ**) **1-9** involved in the present study.

2. Experimental section

2.1. Photophysical studies

Some absorption and emission parameters in phosphate-buffered (PB, pH 7.3) and ethanol have been determined for dyes **SQ1-4** and **SQ7**. The preparation of the phosphate buffer with a concentration of 0.05 M and pH 7.3 was carried out from $Na_2HPO_4 \cdot 7H_2O$ (2.270 g) and NaH_2PO_4 (0.565 g) which were dissolved in 500 mL of ultrapure water. To obtain the absorption spectra, a Lambda 25 UV/Vis spectrophotometer (Perkin Elmer, Waltham, United States of America), operating between 500-900 nm and at room temperature (r.t.) was used. The emission measurements were carried out using a Varian Cary Eclipse fluorescence spectrophotometer (Agilent Technologies, Santa Clara, United States of America) which was programmed to work with 10 nm slits for excitation and emission and an excitation wavelength (λ_{exc}) of 580 nm.

Trough equation 1 and using zinc phthalocyanine (ZnPh, Φ_F = 17% in dimethylformamide (DMF)) [26] as reference the relative fluorescence quantum yields (Φ_F) were calculated.

$$\Phi_F = \Phi_{Fref}\left(\frac{F_{dye}}{F_{ref}}\right)\left(\frac{A_{ref}}{A_{dye}}\right)\left(\frac{n^2_{media}}{n^2_{DMF}}\right) \quad (1)$$

where the Φ_F is the relative fluorescence quantum yield, F is the integrated emission intensity, A the absorbance, n is the refractive index. The subscripts *dye* and *ref* are relative to the dye and reference, respectively.

2.2. Photosensivity study

Dyes **SQ1**-**4** and **SQ7** were dissolved in dimethylsulfoxide (DMSO) in order to obtain solutions with a concentration of 1 mM that were later diluted in PB to a concentration of 25 μM. In a quartz cuvette and under continuous agitation, each solution was subjected to irradiation for 20 minutes using a lamp with emission in the UV/Vis region and a power of 150 W. At each minute, measurements of absorption between 500-800 nm were obtained using a Cary 50 Bio spectrophotometer.

2.3. Dyes' singlet oxygen ($^1O_2$) production ability

To assess the capacity of dyes to generate singlet oxygen, DMSO solutions of dyes **SQ1-4** and **SQ7** and methylene blue with a concentration of 6.7×10^{-4} M and a 1 mM DMSO solution of 1,3-diphenylisobenzofuran (DPBF) were prepared and then diluted in DMSO or PB in order to obtain a concentration of 20 mM and 0.1 mM, respectively. In a 96-well microplate each solution was added in quadruplicate and irradiated with a light emitting diode (LED) system centered at 653 nm. Using a spectrophotometer, absorbance measurements were taken at 410 nm after each irradiation interval up to a total irradiation time of 600 seconds.

2.4. Antifungal activity assays

Saccharomyces cerevisiae PYCC 4072 was used as a biological model for the evaluation of the antifungal performance of dyes **SQ1**-**4** and **SQ7**. Using a broth microdilution method (M27-A3, CLSI – *Clinical and Laboratory Standards Institute*) [27], the minimum inhibitory concentration (MIC) of dyes, the concentration that causes an >80% decrease in yeast growth, was determined. For each experiment a fresh culture was prepared in YPD agar plates and then diluted in Roswell Park Memorial Institute (RPMI) 1640 medium, buffered to pH 7.0 with 0.165 M morpholenepropanesulfonic acid (MOPS) in order to obtain

a concentration of 2.25×10^3 cells/mL that was cultivated in 96-well microplates. Dyes solutions in DMSO with a concentration of 10 mM were dissolved in RPMI 1640 medium and added to each well to have a dye concentration of 0, 6.25, 12.5, 25, 50 and 100 μM and a DMSO concentration of 0.5 % (v/v) per well. After preparation of the plates, two experimental conditions were applied, some plates were protected from ambient light and the others subjected to irradiation for 30 minutes using an LED system and then incubated for 48 hours, at 30 °C. A LED system with an emission wavelength centered at 653 nm, radiant flux of 3.8 ± 0.3 mW, irradiance of 5.4 ± 0.5 mW/cm^2 and a fluence of 9.7 J/cm^2 for an exposure time of 30 minutes was used. Through absorbance readings at 640 nm in a microplate photometer (Molecular Devices SpectraMax Plus) it was possible to assess the state of cell growth. The assays are performed in triplicate in at least two independent experiments.

2.5. Evaluation of squaraine dyes intracellular distribution

Agar plates with YEPD (1% yeast extract, 2% peptone, 2% glucose) medium are used to grown new cultures of *Saccharomyces cerevisiae* W303-1A strain for each experiment performed. From this culture and using liquid YEPD medium, cell suspensions were prepared and subsequently incubated at 30 °C and 120 rpm in a Certomat H incubator, in order to reach an optical density between 0.5-0.6 at a wavelength of 640 nm. Solutions of each dye (50-100 μM) in DMSO and 4′,6-diamidino-2-phenylindole (DAPI) (0.2 mg/ml) were added to aliquots of this suspension and incubated for 30 minutes at 30° C. After this time cells are centrifuged for a period of 3 minutes and 3000 rpm. The resulting pellet was resuspended in 20 μL of PBS and prepared for observation on a Leica MicrosystemsDM-5000B microscope with 100× oil immersion objective and properly adjusted red, blue, green and differential interference contrast (DIC) filters.

All images shown were obtained from a Leica DFC350 FX Digital Camera and processed with LAS AF Microsystems software. Control assays were performed only with the addition of DMSO in order to analyze if this solvent affect the cellular morphology. The images presented are the representative result of three independent experiments.

2.6. Dye-protein interaction assays

To analyze the potential use of dye **SQ7** as fluorescent probe for protein detection, a DMF stock solution of dye (6.7×10^{-4} M) and a HSA solution (14 mM) in PB were prepared.

A protocol that allowed to keep the dye concentration constant (2 μM) varying the HSA concentration (0-3.5 μM) was applied and after 1 hour of incubation the fluorescence intensity was measured, using a Varian Cary Eclipse fluorescence spectrophotometer (Agilent Technologies, Santa Clara, United States of America) programmed to work with an excitation slit of 5 nm, an excitation slit of 10 nm and an excitation wavelength of 580 nm.

2.7. Binding and sensing parameters determination

Some binding parameters of dye **SQ7** after interaction with HSA were determined.

Through the Benesi-Hildebrand equation (Equation 2)[28]:

$$\frac{1}{F_X - F_0} = \frac{1}{F_\infty - F_0} + \frac{1}{K_b\,(F_\infty - F_0)}\left(\frac{1}{[HSA]}\right) \quad (2)$$

where F is the fluorescence intensities and the subscripts 0, x e ∞ are relative to the absence of HSA, the presence of a given concentration of HSA, and the concentration at which a complete interaction occurs, respectively, was possible obtained the binding constant (Kb).

To determine the dissociation constant (K_d) and the Hill coefficient (n_H) equation 3 was applied:

$$log\,\frac{Q}{1-Q} = n_H log[HSA] - logK_d \quad (3)$$

where $Q = F/F_{max}$, is the fraction of sites occupied with the HSA.

Bases on equation 4 ($DL = 3\sigma/k$) and equation 5 ($QL = 10\sigma/k$), where σ is the standard deviation of blank and k is the slope between the fluorescence intensity and protein concentration, it was possible to determined sensitivity (S), detection limit (DL) and quantification limit (QL).

3. Results and discussion

3.1. Photophysical studies

Fundamental photophysical studies of squaraine dyes **SQ1**-**4** and **SQ7** were carried out in ethanol and phosphate buffer and the results are present in Table 1 and Figure 2. Photophysical studies, in this solvents, of dyes **SQ5, 6** and **SQ8, 9** dyes have been recently reported in the literature [25].

In ethanol, the dyes showed maximum absorption wavelengths (λ_{abs}) between 635-649 nm and maximum emission wavelengths (λ_{em}) between 655-663 nm, with moderate stokes shifts ($\Delta\lambda$ = 14-24 nm) being obtained. The pattern of absorption and emission is similar to other dyes of this family already studied, with sharp and narrow bands being obtained in an organic solvent. Also, the high molar extinction coefficients ($\mathcal{E}$) between 1.04×10^5 - 1.99×10^5 M^{-1} cm^{-1} obtained for the studied dyes are characteristic of this class of dyes. The structural changes of the **SQ1**-**4** dyes did not cause significant changes in the absorption and emission wavelength since they present very similar values with a variation of only 1 nm in the absorption values and 3 nm in the emission values.

To obtain the values of the relative fluorescence quantum yields a DMF solution of zinc phthalocyanine was used as reference. Dye **SQ7** showed the highest value with a value exceeding 100%, followed by dye **SQ4** (30.1%), **SQ3** (26.6%), **SQ2** (24.3%) and **SQ1** (23.9%).

Regarding the photophysical assays in PB, absorption and emission wavelengths between 633-654 nm and 648-712 nm, respectively, were obtained. The λ_{abs} and λ_{em} of the **SQ1**-**4** dyes in PB are already reported in the literature [23, 24]. In the present study, complementary studies were carried out, such as the determination of molar extinction coefficients and the relative fluorescence quantum yield in this solvent. In aqueous medium the **SQ1**-**4** dyes showed higher absorption and emission wavelengths than those obtained in ethanol, with values between 645-712 nm respectively. The **SQ7** dye showed a different behavior from the other dyes, presenting lower absorption and emission wavelengths in PB (633-648 nm) than those obtained in ethanol.

205 **Table 1.** Some photophysical features of squaraine dyes **SQ1-4 and SQ7** in ethanol and phosphate buffer.

Solvent		Squaraine dye				
		SQ1	**SQ2**	**SQ3**	**SQ4**	**SQ7**
EtOH	**λ_{abs} (nm)**	636	635	635	635	649
	λ_{em} (nm)	660	657	656	655	663
	$\Delta\lambda$ (nm)	24	22	21	20	14
	ε (M^{-1} cm^{-1})	1.98×10^5	1.99×10^5	1.64×10^5	1.86×10^5	1.06×10^5
	Φ_F (%)	23.9	24.3	26.6	30.1	>100
PB	**λ_{abs} (nm)**	650*	645*	654**	650*	633
	λ_{em} (nm)	708*	700*	712**	708*	648
	$\Delta\lambda$ (nm)	58*	55*	58	58*	15
	ε (M^{-1} cm^{-1})	4.31×10^4	5.76×10^4	4.17×10^4	6.61×10^4	4.71×10^4
	Φ_F (%)	1.95	1.46	1.26	1.63	>100
RPMI	**λ_{abs} (nm)**	659	660	673	655	628

206 *[23]; **[24].
207 ** excitation and emission slit of 10 nm, λ_{exc} 580 nm,

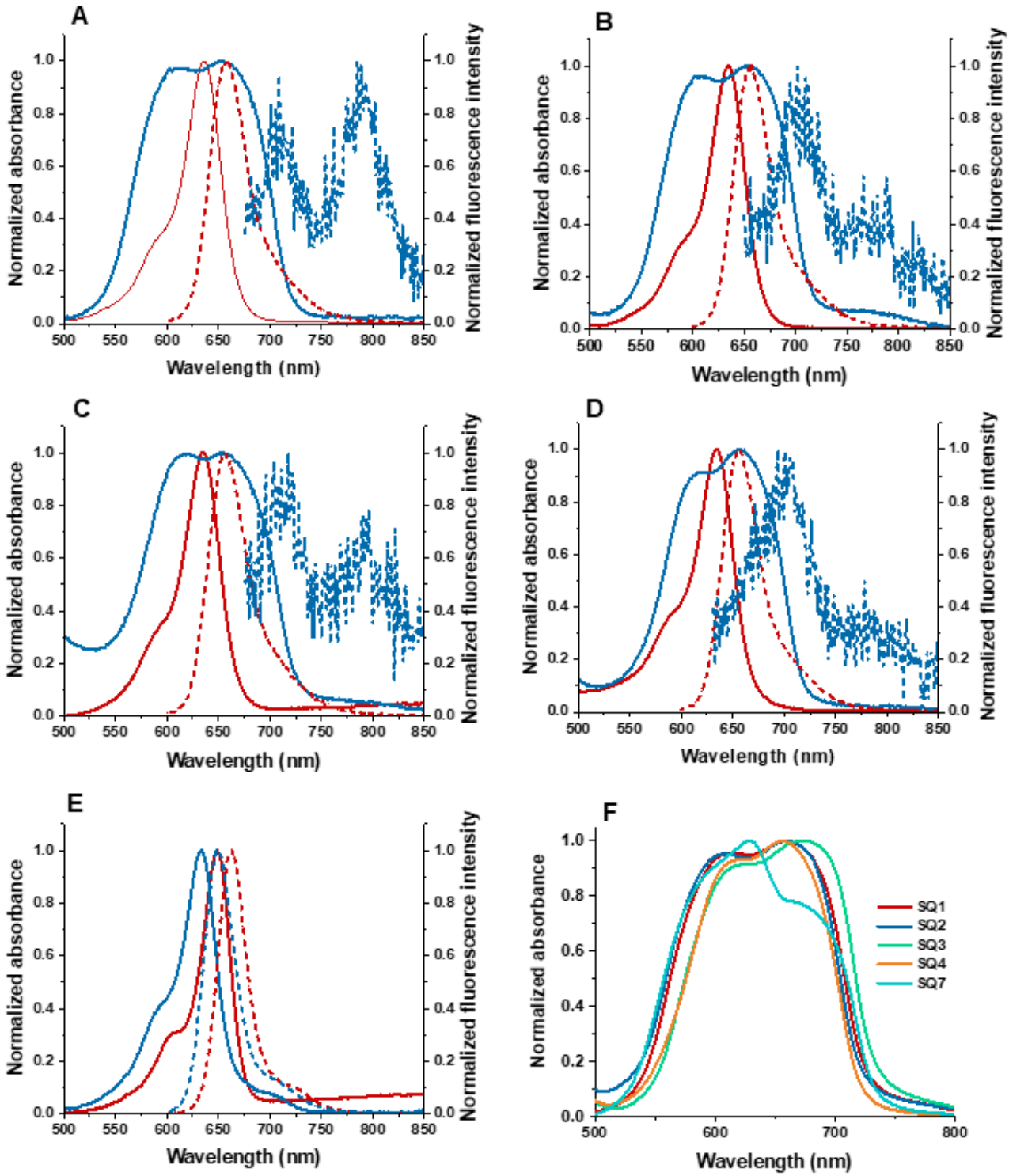

Figure 2. Absorption (solid lines) and emission (dash lines) pattern of **SQ1-4** and **SQ7,** A, B, C, D and E, respectively, in ethanol (—) and PB (—). F- Absorption spectra of **SQ1-4** and **SQ7** in RPMI.

Through the analysis of Figure 3 (dash lines) it is possible to verify that the absorption spectra in PB of the dyes **SQ1**-**4** and **SQ7** present a band overlapping bands, one assigned to the monomer and other related to aggregates. *H*-aggregates and *J*-aggregates [29] are the type of aggregates that can formed and to realize which type is present in the aqueous solutions of the dyes tested, an absorption spectrum was obtained with the addition of Triton X-100. This reagent is a surfactant that prevent the formation of aggregates, thus making it possible to observe only the peak relative to the monomer. These tests revealed that the band positioned at greater wavelength is relative to the monomer band, and the other at a shorter wavelength can be attributed to H-aggregates. The low fluorescence quantum yields obtained in PB (1.26-1.95%) for dyes **SQ1**-**4** are due to the high insolubility and therefore a strong tendency to form *H*-aggregates, known as non-fluorescent aggregates. However, for the dye **SQ7**, the fluorescence quantum yield, as occurred in ethanol, exceeds 100%, which is related to the higher solubility of the dye in PB and a lower trend to form non-fluorescent aggregates. It is possible to observe in Figure 3E (dash line) that there seems to be a small band to the right of the monomer band that could indicate the formation and *J*-aggregates. These aggregates are characterized by emitting fluorescence, which may also be contributing to the high fluorescence quantum yield obtained for dye **SQ7**.

The absorption wavelengths in RPMI (Figure 2F, Table 1) were determined in order to choose the most suitable wavelength to perform the irradiation in biological assays. The absorption profile is similar to that obtained in PB with only small variations in the absorption wavelength value.

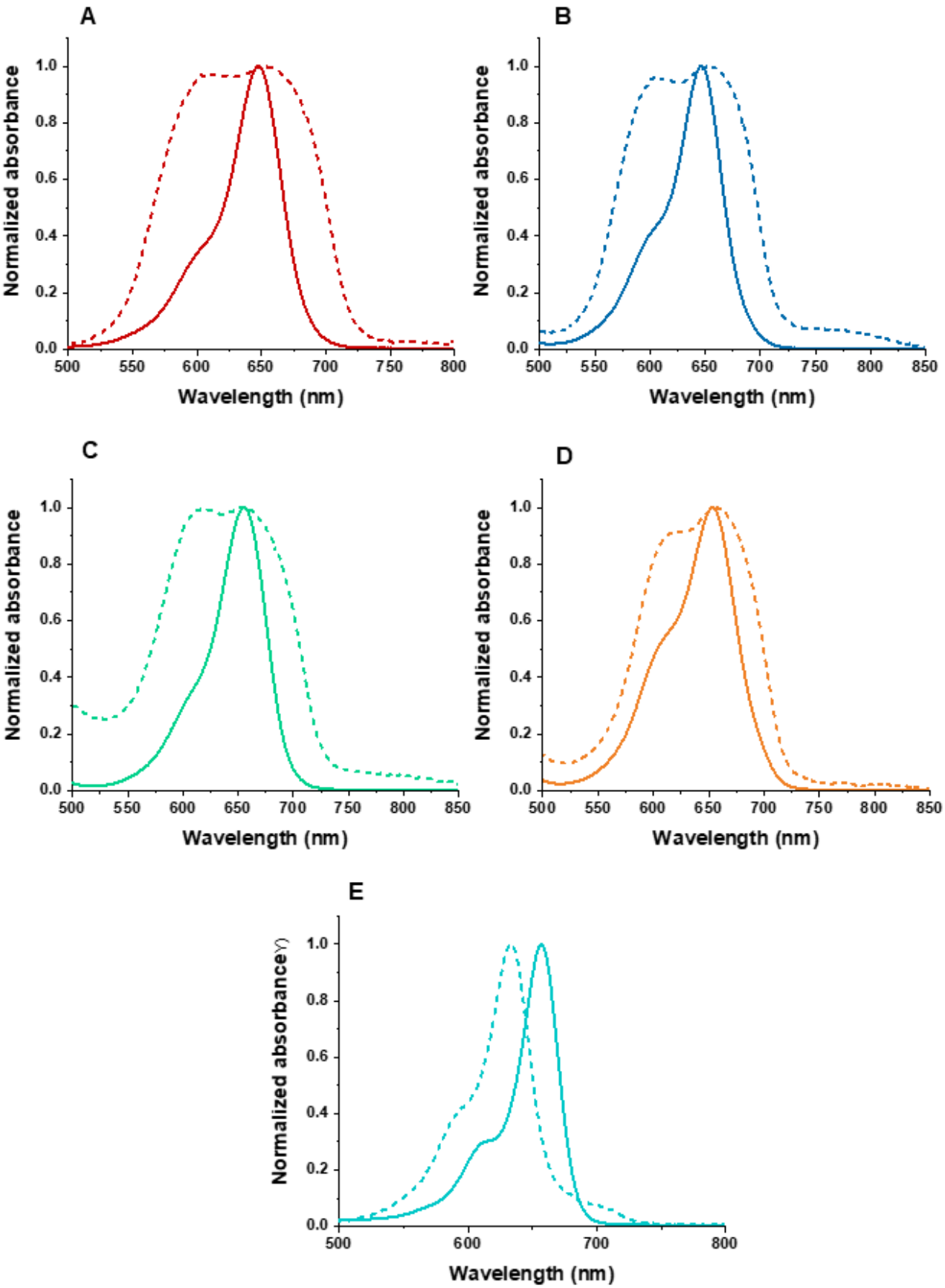

233

Figure 3. Absorption spectra of dyes **SQ1-4** and **SQ7** in PB, A, B, C, D and E, respectively, in absence (dash lines) and presence (solid lines) of Triton X-100.

3.2. Photostability analysis

Photostability is an important parameter that must be evaluated in order to understand what effect light has on a substance [30]. The objective is to understand if, when irradiated, this substance undergoes changes or even forms photoproducts that will affect or contribute to its effectiveness. Photostability was studied in PB to simulate the behavior of dyes in biological media and the results obtained were compared with those obtained for methylene blue (tested under the same conditions) known for its high resistance to photodegradation. A lamp with a power of 150 W and emission in the UV/Vis region was used and the results are shown in Figure 4.

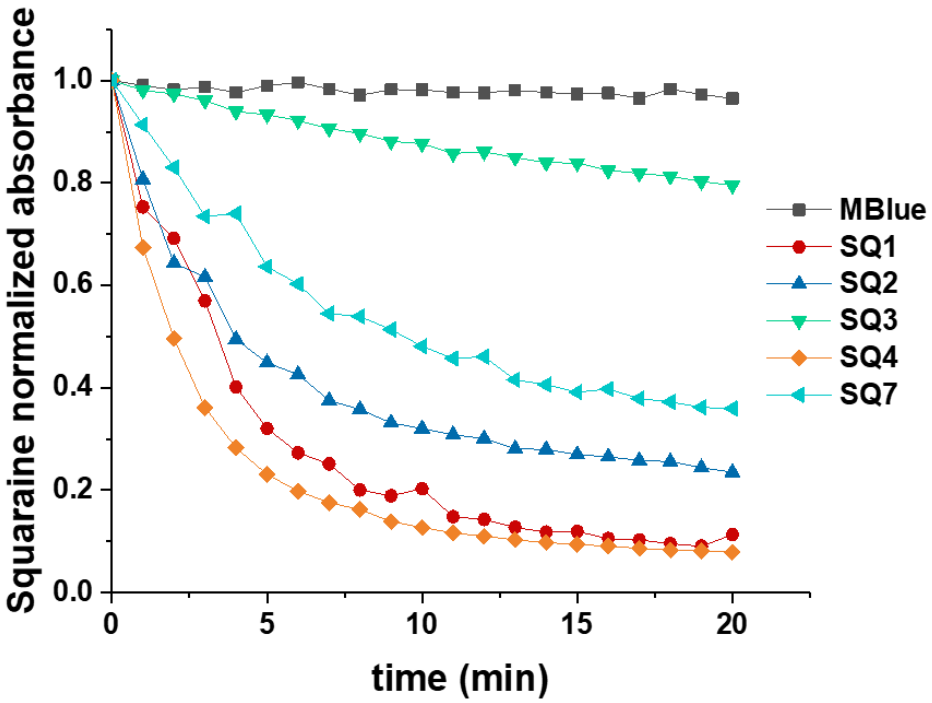

Figure 4. Photostability of **SQ1-4** and **SQ7** and MBlue in PB as a function of irradiation time (min).

Among the **SQ1-4** squaraine dyes, all derived from indolenin, the dye with a dimethylbarbituric acid group in the central ring (**SQ3**) proved to be the most photostable with only a small decrease in its absorbance. This dye demonstrated a light response similar to the benzo[*e*]indole-derived dye **SQ6** and indolenine derived dye **SQ8** whose photostability was already reported by Gomes *et al*. [25]. The lower

photostability is attributed to dye **SQ1** and **SQ4**, which was almost completely degraded, losing their ability to emit color, as observed for dyes **SQ5** and **SQ9**. Comparing dye **SQ1** with **SQ2** it is possible to verify that the substitution of an oxygen atom for a sulfur atom contributed to a small improvement in photostability. Observing the results of dye **SQ1** and **SQ3**, the great difference that occurs in terms of photostability is evident, proving that the replacement of hydrogen atoms by methyl groups is quite favorable for the photostability of the dye. This may be related to the hydrophobic character of the methyl groups that make the dye **SQ3** less soluble in aqueous media, that is, it has a weak interaction with the water presence, which allows it to maintain its stability in this environment. The opposite occurs with dye **SQ1**, in which the presence of the hydrogen atom instead of the methyl group makes the dye more soluble in aqueous media and, consequently, less stable.

Dye **SQ1** and **SQ5** are analogs, one derived from indolenine and the other is derived from benzo[*e*] indole. This structural change does not seem to significantly affect photostability. The same happens with the dyes **SQ2** and **SQ6**, however in this case the dye derived from benzo[*e*]indole (**SQ6**) proved to be much more photostable.

This proves that the photostability parameter is not only related to the introduction of a specific substituent group but to the different combination of substituents that the molecule presents.

3.3. Singlet Oxygen Formation Ability

The ability of **SQ1**-**4** and **SQ7** dyes to produce singlet oxygen was evaluated by performing a DPBF assay. This reagent strongly absorbs at 410 nm and when interacting with the singlet oxygen generated by the irradiation of the dyes, breaks its π-system forming a colorless compound, incapable of absorbing and emitting light [31]. To evaluate qualitatively the singlet oxygen generation of the squaraine dye, the DMSO solutions of dyes and DPBF (Figure 5A) and PB (Figure 5B) was irradiated with a LED system with an emission at 660 nm and the absorbance at 410 nm monitored. This parameter was evaluated in DMSO and also in PB to mimic the biological conditions. Methylene blue was used for comparison as its ability to generate singlet oxygen is already known [32].

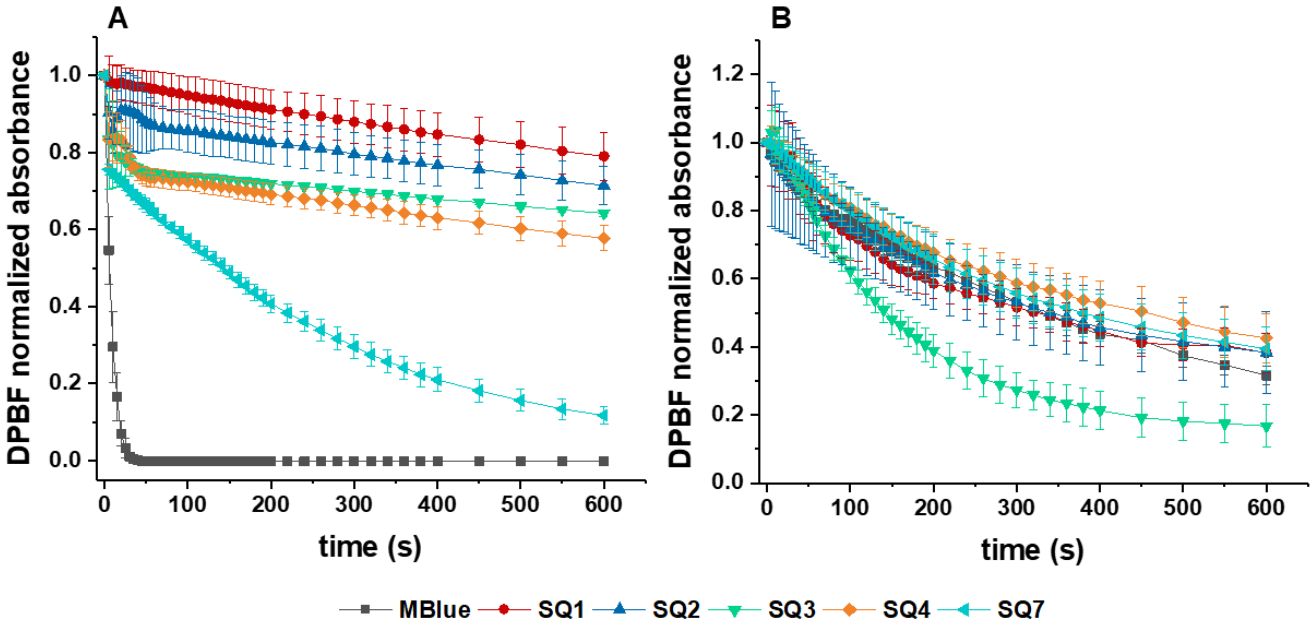

278

279 **Figure 5.** Decay of the 1,3-diphenylisobenzofuran (DPBF) 410 nm-absorbance in presence of **SQ1-4** and
280 **SQ7** and MBlue in DMSO (A) and PB (B). Data are presented as mean ± standard deviation as a result of
281 experiments performed in quadruplicates.

282

283 In DMSO, as expected, methylene blue leads to an almost instantaneous decay of DPBF (after 30s of
284 irradiation). The dye **SQ7** proved to be the most efficient in the production of singlet oxygen, causing a
285 DPBF degradation of more than 80% after 600 seconds of irradiation. The barbiturate derivatives showed
286 a similar behavior with dye **SQ4** showing slightly higher singlet oxygen production than their analogues.
287 In PB the **SQ1-4** dyes improved their ability to generate singlet oxygen, causing a greater degradation of
288 DPBF than that observed in DMSO. Once again, the results for these dyes are very similar to each other,
289 highlighting the dye **SQ3** with a decrease in DPBF absorbance of more than 80%. In aqueous medium, the
290 **SQ3** dye obtained a result similar to that already reported for the **SQ8** dye [25], being the dyes most
291 efficients in terms of singlet oxygen production.

292 The greater or lesser efficiency in the production of singlet oxygen is related to the solubility and
293 stability that a given compound presents in different solvents, which in turn is influenced by the different
294 substituents present in each dye. In the case of **SQ3** it improved its activity in PB while the **SQ7** dye

decreased its capacity to generate singlet oxygen also in PB. The results are in agreement with the results obtained in the photostability where it was observed that the presence of the methyl groups of the dye **SQ3** contributed to the good photostability of the dye, most likely due to the type of interactions that the dye established with the medium. Dye **SQ7** proved to be significantly more efficient in the DMSO assays, perhaps because it has a high solubility that allows it to establish some kind of interaction with the medium, which favors the production of singlet oxygen. The opposite occurs in PB, where this dye diminishes its ability to generate singlet oxygen.

3.4. Antifungal activity

To test the potential of the dyes as antifungal agents, assays were performed using the *Saccharomyces cerevisiae* PYCC 4072 strain. Through the application of a broth microdilution method, five concentrations of dyes (0, 6.25, 12.5, 25, 50, 100 μM) were tested in an attempt to determine which of the concentrations corresponds to the MIC, the concentration responsible for limiting growth by at least 80% compared to a condition without dye. Table 2 compiles the MIC values obtained in the dark and after irradiation and the logarithms of the partition coefficient (Log *P*) theoretically obtained through structural analysis with an appropriate software [33].

For dye **SQ1** the lowest MIC value was obtained, 25 μM, followed by dye **SQ2** with an MIC of 50 μM and by dyes **SQ3** and **SQ4** with an MIC of 100 μM. The concentrations tested did not allow determining the MIC value of the dye **SQ7**, and it was not possible to test higher concentrations due to the limited solubility of the dye. Dyes **SQ1**-**4** and **SQ7** are all derived from indolenine, and it is possible to verify that alterations only at the level of the four-membered central ring led to different response to the light and consequently to a different antifungal activity of the dyes.

The squaraine dyes are known for their photosensitizing activity, so tests were carried out with irradiation to try to understand if it improves the antiproliferative activity. The LED system with emission at 653 nm used was composed of several LEDs, each one illuminating a single well of the microplate. The microplates were irradiated for 30 minutes, which corresponds to an irradiation dose of 9.7 J/cm^2.

Table 2. Antifungal performance of dyes **SQ1**-**4** and **SQ7** against *Saccharomyces cerevisiae* PYCC 4072 strain and the respective MIC values and Log *P* values. MIC values are present in μM.

Dye	MIC (dark) (μM)	MIC (irrad) (μM)	Log P
SQ1	25	50	3.30
SQ2	50	>100	3.65
SQ3	100	50	3.44
SQ4	100	50	6.33
SQ7	>100	50	2.61

The results showed that irradiation improved the activity of **SQ3** and **SQ4** dyes, with a decrease in the MIC to 50 μM, half the concentration obtained in the assays carried out in the dark. Due to the irradiation is possible to obtain a MIC value for the dye **SQ7** (50 μM), which was not possible under conditions of absence of light.

The **SQ1** and **SQ2** dyes increased the MIC value after irradiation, which could be related to the fact that the light causes the dyes to degrade and they lose their antifungal properties at the concentrations tested. These results are in agreement with those obtained in the photostability tests in which both dyes were shown to be quite photounstable. The introduction of barbiturate groups in the dyes **SQ1** and **SQ2** did not prove to be advantageous in terms of increasing the photosensitizing capacity of the dyes. Dye **SQ4** also showed a low resistance to photodegradation, but in the light tests this dye proved to be more effective than in the dark tests, which may be related to the fact that the dye, in response to light absorption, produces subproducts with a greater antiproliferative capacity. Dye **SQ3** presented the same results as **SQ4**, but in the photostability test it revealed a good light tolerance, suffering little photodegradation, which will indicate that its antifungal activity is due to its structure and there is no formation of secondary products.

In the dark, the better antiproliferative capacity, is attributed to the **SQ1**. As already mentioned in the photostability tests, the different structure of the dyes, with the different substituents, will influence their different response to light, being able to attribute to the dyes a greater or lesser photostability. The same

342 can be observed in the antifungal activity tests in which it was possible to verify different responses of the
343 dyes in the tests carried out in the dark and after irradiation. It is the different structural changes that will
344 give a more lipophilic or hydrophilic character to the dye molecules, and thus influence the way these
345 molecules interact with the environment that surrounds them and consequently the response they will give.
346 Log P values range from 2.61-6.33 and correspond to an estimated value of the dye's hydrophobicity.
347 Low Log P values are attributed to more water-soluble compounds and higher values to compounds with a
348 greater affinity for the cell membrane. In this case, the differences between the obtained Log P values do
349 not allow correlation with the MIC values.
350
351 **3.5. Fluorescence microscopy assays**
352 The location of dyes at the cellular level is essential in understanding the possible mechanisms of
353 action, also related to their greater or lesser effectiveness in various biological applications. The squaraine
354 dye's cellular location is not only a result of the heterocyclic groups presents but also of the entire
355 combination of substituents of the dye structure.
356 Colocalization experiments were performed using DAPI, a probe that allows the labeling of organelles
357 with high DNA content, nuclei, and mitochondria. Our colocalization results suggest that squaraine dyes
358 derived from indolenine with a barbituric (**SQ1**), thiobarbituric (**SQ2**) and dimethylbarbituric (**SQ3**)
359 accumulate preferentially in mitochondrial web and perinuclear membrane. The introduction of two phenyl
360 groups into the thiobarbiturate group led dye **SQ4** to accumulate in the cell vacuole. The dye derived from
361 benzo[*e*]indole with a thiobarbituric fraction (**SQ6**) and the dye benzo[*e*]indole-based with an ester group
362 in the *N*-chain (**SQ9**) also demonstrated a preferential accumulation in cells vacuole. The weak staining
363 intensity will be due to their low solubility in a biological medium.
364 Comparing the barbiturated benzo[*e*]indole-based dyes, it is possible to verify that the dye with the
365 barbiturate group (**SQ5**) is distributed throughout the perinuclear membrane and the dye with the
366 thiobarbiturate group (**SQ6**) is colocalized in cell vacuoles. This different cellular distribution is only
367 related to the substitution of an oxygen atom for a sulfur atom.

Dyes **SQ7** and **SQ8**, both derived from indolenine and varying only in the *N*-chain substituents, showed a similar distribution pattern with an accumulation in the perinuclear membrane and also in a cellular structure that could not be identified.

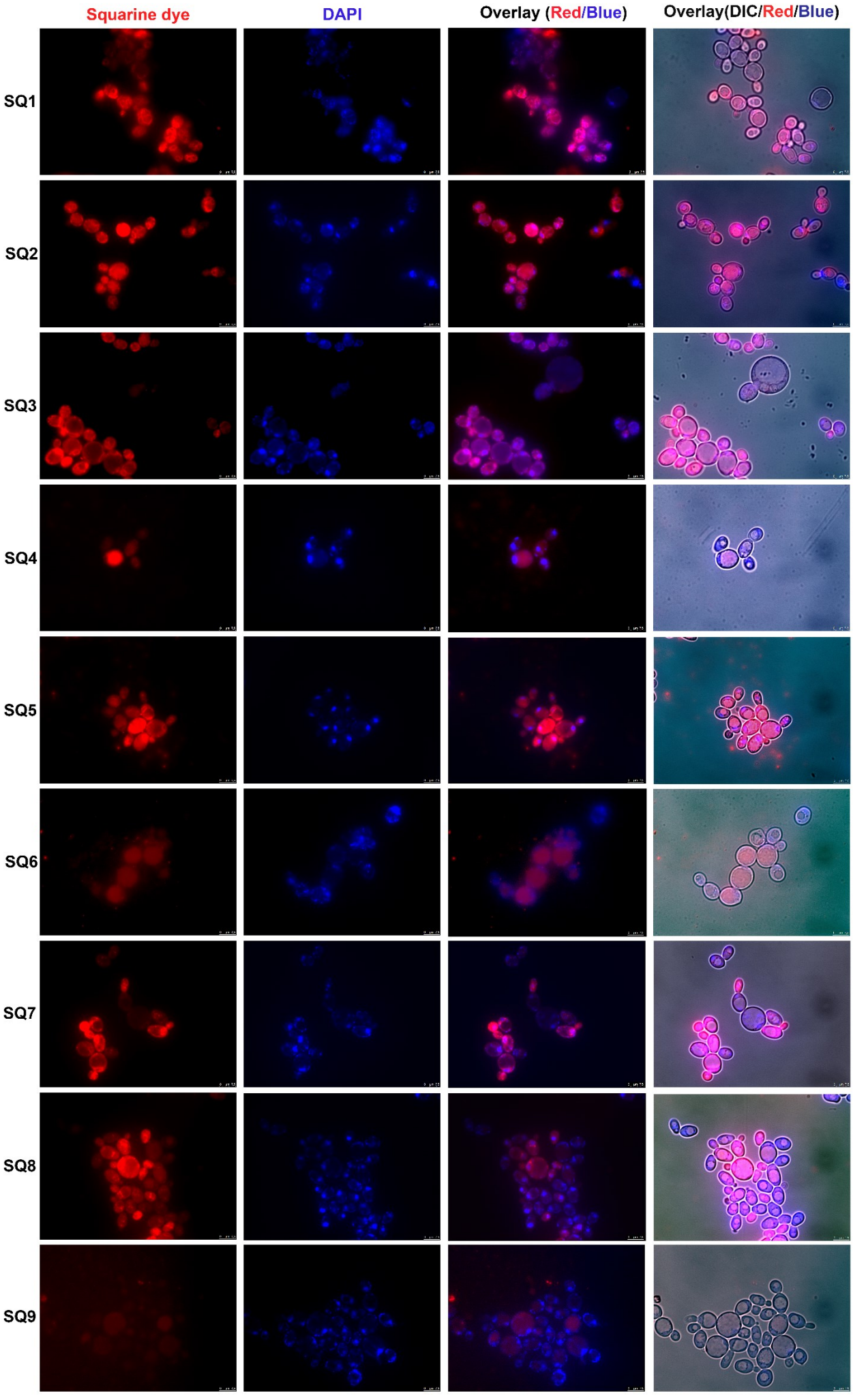
Squarine dye
DAPI
Overlay (Red/Blue)
Overlay(DIC/Red/Blue)
SQ1
SQ2
SQ3
SQ4
SQ5
SQ6
SQ7
SQ8
SQ9

373

Figura 6. Intracellular distribution of **SQ1-9** after incubation with **SQ1-3**, **5**, **7**, **8** (50 μM) and **SQ4**, **6**, **9** (100 μM) at 30° C for 30 minutes. Images were obtained at 100× magnification.

3.6. HSA interaction studies

Interaction studies were performed between dye **SQ7** and HSA to ascertain its potential application as a fluorescent probe for the detection of this protein. Dyes **SQ1-6** and **SQ8-9** have already been studied in terms of interaction with HSA [23-25], and now only studies with **SQ7** are carried out so that a comparison of the results can be made.

As observed for other squaraine dyes, an increase in fluorescence intensity is the response to increased concentration of HSA (Figure 7A). In the case of the **SQ7** dye, a bathochromic shift of the maximum emission wavelength of about 20 nm, between emission in the absence of HSA and in the presence of 3.5 μM HSA is revealed. The increase in fluorescence intensity with the increase of protein concentration is described by a linear function presenting a square of correlation coefficient (R^2) very close to unity (Figure 7B).

From the Benesi–Hildebrand equation (Equation 2) it is possible to plot a graph of $1/(F_x-F_0)$) against 1/[HSA] from which the binding constant is calculated (Figure 7C). A binding constant of 3.25×10^5 M (Table 3) was obtained, whose order of magnitude indicates the high affinity between the dye and the protein. The Benesi–Hildebrand plot also provides information on the stoichiometry of complexation between dye and protein, which in this case suggests 1:2 due to the non-linear trend of the plot.

The graph obtained through equation 3 was plotted in an attempt to obtain the dissociation constant and the Hill constant, which was not possible due to the fact that the graph (Figure 7D) obtained is not linear, as already reported in other articles by some of us [23-25]. However, it is possible to draw other conclusions about the mode of binding of the dye to the protein that is related to the various binding sites that HSA makes available for the dye. Depending on the structure of the dye, it will bind to different sites with different affinities, that is, the dye has a higher affinity for a particular binding site and will only bind to another site after the first one is saturated. This will lead to each binding site having a different dissociation constant depending on the concentration of dye that reacts with the protein [34].

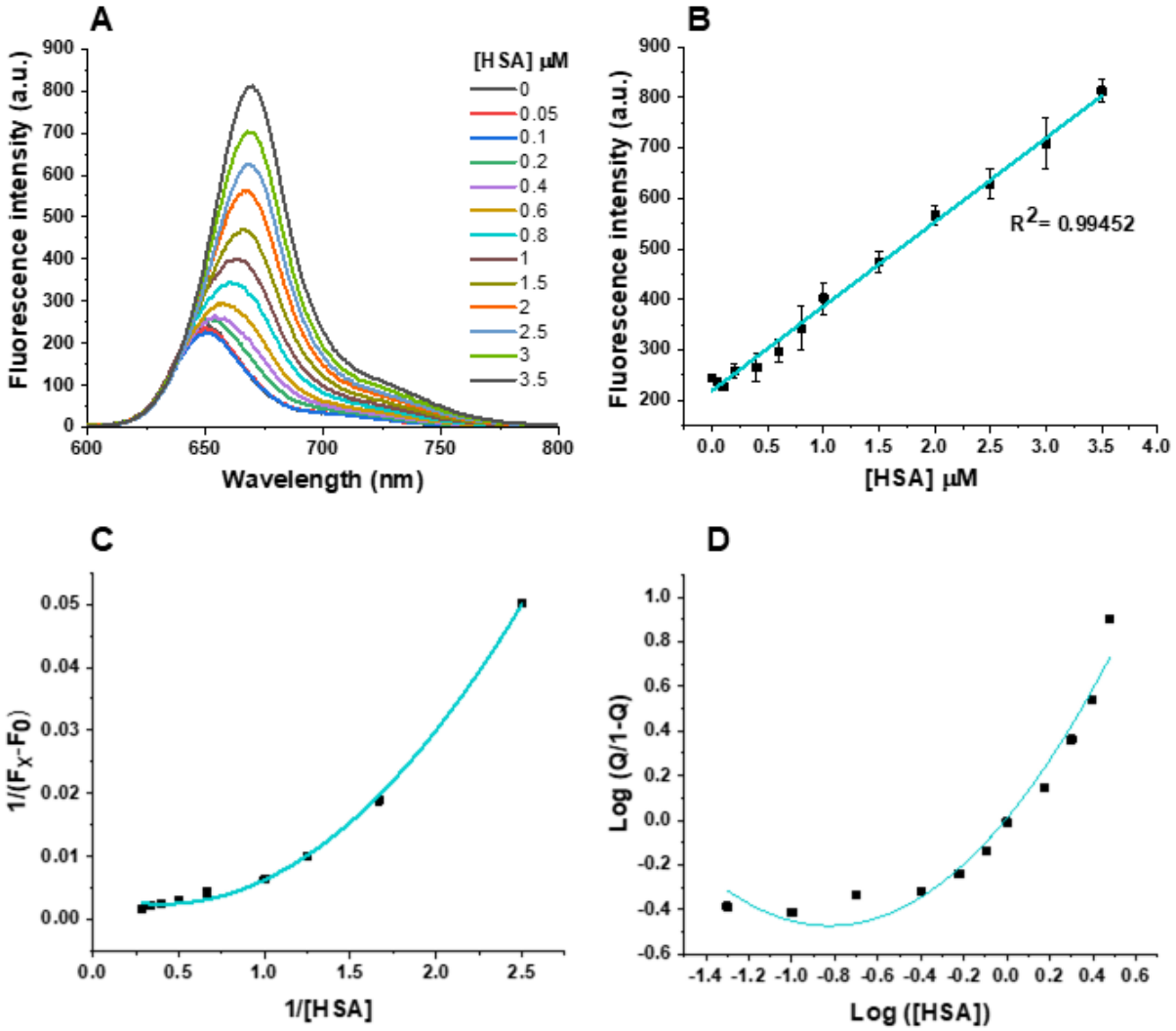

Figure 7. **A**- Fluorescence spectra of **SQ7** after one hour of incubation with different concentrations of HSA (0-3.5 µM). **B**- Linear correlation between fluorescence intensity and protein concentration with the respective square of the correlation coefficient (R^2). **C**- Benesi-Hildebrand plot for the binding of squaraine dye **SQ7** with HSA. **D**- Hill's plots obtained for the interaction of squaraine dye **SQ7** with HSA. The fluorescence intensity values obtained result from the application of an excitation slit of nm and an emission slit of 10 nm and an excitation wavelength of 580 nm.

Table 3 presents some parameters resulting from the dye-protein interaction studies. In the absence of BSA a fluorescence intensity (**F_0**) of 244.24 a.u. was reached, after addition of a concentration of 3.5 µM of HSA the fluorescence intensity value (F) was 812.96 a.u.. The **SQ7** dye showed the highest fluorescence

intensity value but as in the absence of HSA the dye showed considerable fluorescence with quantum yields of fluorescence exceeding 100% the difference between values resulted in an increase rate of only 3-fold, the lowest among dyes **SQ1**-**6**,**8**,**9**. Fluorescence linear response of dye to the increasing amounts of HSA is an extremely relevant factor with regard to the use of squarylium dyes as a quantitative fluorescent probe. The detection limit and quantification limit of 113 nM and 376 nM, respectively, are within the order of magnitude of those obtained for the other dyes, with the best value assigned to the dye **SQ3** with DL of 51 nM and QL of 171 nM [24], which indicates a greater sensitivity to variations in HSA concentration.

Table 3. Some parameters obtained for the interaction between dye **SQ7** and HSA. F_0 is the fluorescence intensity of dye in absence of HSA, F is the fluorescence intensity of dye at the highest concentration of HSA, F/F_0 is the ratio between these last two parameters.

Dye	F_0 (a.u.)	Dye-protein complex fluorescence properties					
		F (a.u.)	F/F_0	S (nM)	DL (nM)	QL (nM)	K_b (M^{-1})
SQ7	244.24	812.96	3.33	1.67×10^5	113	376	3.25×10^5

4. Conclusions

A comparison study was carried out between dyes derived from benzo[*e*]indole and indolenine regarding their application as antifungal agents and fluorescent probes. The synthesis of the dyes referred here as well as some of the studies discussed has already been published, however it is referred here to complement the studies and to be able to make a comparison under the influence of the different structure of the dyes in the applications evaluated.

The tendency of dyes to form aggregates in aqueous media coincides with all dyes and the tests carried out with the addition of Triton X-100 showed that the aggregates formed are responsible for the dyes presenting low fluorescence quantum yields in PB.

Considering the photosensitive character attributed to the squarylium dyes class, it has been shown that small structural changes lead to considerable differences in the response of dyes to light.

The dyes ability to generate singlet oxygen is directly related to the good performance of the dyes as photosensitizers and all dyes showed to be able to generate this reactive species in a more or less efficient way depending on the dye structure. However, it was not possible to relate the efficiency in producing singlet oxygen with the performance of the dyes as antifungal agents, perhaps due to the different solubilities and also the different affinity of the dyes to the various cell structures.

Antifungal assays led to obtaining MIC values between 25->100 μM and trough irradiation with adequate wavelength, it was possible to improve the performance of some of the dyes, while in other dyes, the inverse effect was observed, a factor perhaps related to photodegradation or solubility in a biological medium.

The colocalization assays showed that small variations in the structure of the dyes lead to their tendency to accumulate in different cellular structures.

Regarding the interaction with HSA, **SQ7** showed a behavior similar to that observed for the other dyes being obtained quantification and detection limit values that validating the possible use of these dye as a method to detect and quantify HSA. All dyes compared showed a moderate to good interaction with HSA, the most abundant protein in human blood, which may suggest that this albumin could be one of the main biotransporters of these dyes in a living system.

Acknowledgements

Our thanks go to Fundação para a Ciência e Tecnologia (FCT), Comissão de Coordenação e Desenvolvimento Regional do Norte (CCDR-N) and FEDER (European Fund for Regional Development)-COMPETEQREN-EU for financial support to the research centers CQ/UM (UIDB/00686/2020), CBMA (UID/BIA/04050/2020), CQ/VR (UID/QUI/UI0616/2019) and CICSUBI (POCI-01-0145-FEDER-007491), as well as PhD grants to V.S.D.G. (UMINHO/BD/43/2016) and J.C.C.F. (SFRH/BD/133207/2017).

5. References

[1] Kauffman, C. A., "*Fungal infections"*, in *Infectious Disease in the Aging: A Clinical Handbook*, D. Normanand T. Yoshikawa, Editors. **2009**, Humana Press: Totowa, NJ. 347-366. https://doi.org/10.1007/978-1-60327-534-7_22.

[2] Chimelli, L. and Mahler-Araújo, M. B., "Fungal infections", *Brain Pathology*, **1997**, *7*, 613-627. https://doi.org/10.1111/j.1750-3639.1997.tb01078.x

[3] Pauw, B. E., "What are fungal infections?", *Mediterr J Hematol Infect Dis*, **2011**, *3*, e2011001-e2011001. https://doi.org/10.4084/MJHID.2011.001

[4] Baltazar, L. M., Ray, A., Santos, D. A., Cisalpino, P. S., Friedman, A. J. and Nosanchuk, J. D., "Antimicrobial photodynamic therapy: an effective alternative approach to control fungal infections", *Frontiers in Microbiology*, **2015**, *6*, https://doi.org/10.3389/fmicb.2015.00202

[5] Dai, T., Fuchs, B., Coleman, J., Prates, R., Astrakas, C., St Denis, T., Ribeiro, M., Mylonakis, E., Hamblin, M. and Tegos, G., "Concepts and principles of photodynamic therapy as an alternative antifungal discovery platform", *Frontiers in Microbiology*, **2012**, *3*, https://doi.org/10.3389/fmicb.2012.00120

[6] Bouz, G. and Doležal, M., "Advances in antifungal drug development: An up-to-date mini review", *Pharmaceuticals*, **2021**, *14*, 1312. https://doi.org/10.3390/ph14121312

[7] Campoy, S. and Adrio, J. L., "Antifungals", *Biochemical Pharmacology*, **2017**, *133*, 86-96. https://doi.org/10.1016/j.bcp.2016.11.019

[8] He, J., Jo, Y. J., Sun, X., Qiao, W., Ok, J., Kim, T.-i. and Li, Z. a., "Squaraine dyes for photovoltaic and biomedical applications", *Advanced Functional Materials*, **2021**, *31*, 2008201. https://doi.org/10.1002/adfm.202008201

[9] Qiao, W. and Li, Z. a., "Recent Progress of Squaraine-based fluorescent materials and their biomedical applications", *Symmetry*, **2022**, *14*, 966. https://doi.org/10.3390/sym14050966

[10] Markova, L. I., Terpetschnig, E. A. and Patsenker, L. D., "Comparison of a series of hydrophilic squaraine and cyanine dyes for use as biological labels", *Dyes and Pigments*, **2013**, *99*, 561-570. https://doi.org/10.1016/j.dyepig.2013.06.022

[11] Kim, S. H. and Son, Y. A., "*18 - Near-infrared dyes"*, in *Handbook of Textile and Industrial Dyeing*, M. Clark, Editor. **2011**, Woodhead Publishing. 588-603. https://doi.org/10.1533/9780857093974.2.588.

[12] Lima, E., Barroso, A. G., Sousa, M. A., Ferreira, O., Boto, R. E., Fernandes, J. R., Almeida, P., Silvestre, S. M., Santos, A. O. and Reis, L. V., "Picolylamine-functionalized benz[*e*]indole squaraine dyes: Synthetic approach, characterization and *in vitro* efficacy as potential anticancer phototherapeutic agents", *European Journal of Medicinal Chemistry*, **2022**, *229*, 114071. https://doi.org/10.1016/j.ejmech.2021.114071

[13] Ilina, K., MacCuaig, W. M., Laramie, M., Jeouty, J. N., McNally, L. R. and Henary, M., "Squaraine dyes: molecular design for different applications and remaining challenges", *Bioconjugate Chem.*, **2020**, *31*, 194-213. https://doi.org/10.1021/acs.bioconjchem.9b00482

[14] Xia, G. and Wang, H., "Squaraine dyes: The hierarchical synthesis and its application in optical detection", *Journal of Photochemistry and Photobiology C: Photochemistry Reviews*, **2017**, *31*, 84-113. https://doi.org/10.1016/j.jphotochemrev.2017.03.001

[15] Santos, P. F., Reis, L. V., Almeida, P., Oliveira, A. S. and Vieira Ferreira, L. F., "Singlet oxygen generation ability of squarylium cyanine dyes", *Journal of Photochemistry and Photobiology A: Chemistry*, **2003**, *160*, 159-161. https://doi.org/10.1016/S1010-6030(03)00203-X

[16] Dereje, D. M., Pontremoli, C., Moran Plata, M. J., Visentin, S. and Barbero, N., "Polymethine dyes for PDT: recent advances and perspectives to drive future applications", *Photochemical & Photobiological Sciences*, **2022**, *21*, 397-419. https://doi.org/10.1007/s43630-022-00175-6

[17] Wei, Y., Hu, X., Shen, L., Jin, B., Liu, X., Tan, W. and Shangguan, D., "Dicyanomethylene substituted benzothiazole squaraines: The efficiency of photodynamic therapy *in vitro* and *in vivo*", *EBioMedicine*, **2017**, *23*, 25-33. https://doi.org/10.1016/j.ebiom.2017.08.010

[18] Lima, E., Ferreira, O., Silva, J. F., Santos, A. O., Boto, R. E., Fernandes, J. R., Almeida, P., Silvestre, S. M. and Reis, L. V., "Photodynamic activity of indolenine-based aminosquaraine cyanine dyes: Synthesis and *in vitro* photobiological evaluation", *Dyes Pigments.*, **2020**, *174*, 108024. https://doi.org/10.1016/j.dyepig.2019.108024

[19] Lima, E. and Reis, L. V., "'Lights, squaraines, action!' – the role of squaraine dyes in photodynamic therapy", *Future Medicinal Chemistry*, **2022**, *14*, 1375-1402. https://doi.org/10.4155/fmc-2022-0112
[20] Ramaiah, D., Eckert, I., Arun, K. T., Weidenfeller, L. and Epe, B., "Squaraine dyes for photodynamic therapy: study of their cytotoxicity and genotoxicity in bacteria and mammalian cells", *Photochem Photobiol*, **2002**, *76*, 672-7. https://doi.org/10.1562/0031-8655(2002)076<0672:sdfpts>2.0.co;2
[21] Yin, R. and R. Hamblin, M., "Antimicrobial photosensitizers: drug discovery under the spotlight", *Current Medicinal Chemistry*, **2015**, *22*, 2159-2185.
[22] Lima, E., Ferreira, O., Gomes, V. S. D., Santos, A. O., Boto, R. E., Fernandes, J. R., Almeida, P., Silvestre, S. M. and Reis, L. V., "Synthesis and *in vitro* evaluation of the antitumoral phototherapeutic potential of squaraine cyanine dyes derived from indolenine", *Dyes and Pigments*, **2019**, *167*, 98-108. https://doi.org/10.1016/j.dyepig.2019.04.007
[23] Gomes, V. S. D., Gonçalves, H. M. R., Boto, R. E. F., Almeida, P. and Reis, L. V., "Barbiturate squaraine dyes as fluorescent probes for serum albumins detection", *J. Photochem. Photobiol. A: Chem.*, **2020**, *400*, 112710. https://doi.org/10.1016/j.jphotochem.2020.112710
[24] Gomes, V. S. D., Boto, R. E. F., Almeida, P., Coutinho, P. J. G., Pereira, M. R., Gonçalves, M. S. T. and Reis, L. V., "Squaraine dyes as serum albumins probes: Synthesis, photophysical experiments and molecular docking studies", *Bioorg. Chem.*, **2021**, *115*, 105221. https://doi.org/10.1016/j.bioorg.2021.105221
[25] Gomes, V. S. D., Ferreira, J. C. C., Boto, R. E. F., Almeida, P., Fernandes, J. R., Sousa, M. J., Gonçalves, M. S. T. and Reis, L. V., "Squaraine dyes derived from indolenine and benzo[*e*]indole as potential fluorescent probes for HSA detection and antifungal agents", *Photochemistry and Photobiology*, **2022**, *n/a*, https://doi.org/10.1111/php.13624
[26] Ogunsipe, A., Maree, D. and Nyokong, T., "Solvent effects on the photochemical and fluorescence properties of zinc phthalocyanine derivatives", *J. Mol. Struct.*, **2003**, *650*, 131-140. https://doi.org/10.1016/S0022-2860(03)00155-8
[27] "CLSI. Reference Method for Broth Dilution Antifungal Susceptibility Testing of Yeasts; Approved Standard—Third Edition. CLSI document M27-A3. Wayne, PA: Clinical and Laboratory Standards Institute; 2008.",
[28] Das, P., Mallick, A., Haldar, B., Chakrabarty, A. and Chattopadhyay, N., "Fluorescence resonance energy transfer from tryptophan in human serum albumin to a bioactive indoloquinolizine system", *Journal of Chemical Sciences*, **2007**, *119*, 77-82. https://doi.org/10.1007/s12039-007-0013-9
[29] Hestand, N. J. and Spano, F. C., "Expanded theory of H- and J-molecular aggregates: The effects of vibronic coupling and intermolecular charge transfer", *Chemical Reviews*, **2018**, *118*, 7069-7163. https://doi.org/10.1021/acs.chemrev.7b00581
[30] Ahmad, I., Ahmed, S., Anwar, Z., Sheraz, M. A. and Sikorski, M., "Photostability and photostabilization of drugs and drug products", *Int. J. Photoenergy.*, **2016**, *2016*, 8135608. https://doi.org/10.1155/2016/8135608
[31] Zhang, X.-F. and Li, X., "The photostability and fluorescence properties of diphenylisobenzofuran", *Journal of Luminescence*, **2011**, *131*, 2263-2266. https://doi.org/10.1016/j.jlumin.2011.05.048
[32] DeRosa, M. C. and Crutchley, R. J., "Photosensitized singlet oxygen and its applications", *Coordination Chemistry Reviews*, **2002**, *233-234*, 351-371. https://doi.org/10.1016/S0010-8545(02)00034-6
[33] Calculation of molecular properties and drug-likeness-Molinspiration cheminformatics software tool (https://www.molinspiration.com).
[34] Stefan, M. I. and Le Novère, N., "Cooperative Binding", *PLoS Comput. Biol.*, **2013**, *9*, e1003106. https://doi.org/10.1371/journal.pcbi.1003106